Molecular Dynamics Simulation of Coal Structure Damage Under the Action of Surfactant

He Chen (LNTUCH0903@163.com)
Liaoning Technical University
Laigui Wang
Liaoning Technical University
Wenbo An
Liaoning Technical University
Na Zhao
Liaoning Technical University

Research Article

Keywords: surfactant, coal, concentration, mechanical strength, structural damage, molecular dynamics simulation

Posted Date: September 24th, 2021

DOI: https://doi.org/10.21203/rs.3.rs-898303/v1

Abstract

An anionic surfactant, sodium dodecyl sulfate (SDS) was used to modify the coal structure. This was done to improve the compactness of the coal structure, promote the damage of coal structure, improve the efficiency of gas drainage, and prevent shock pressure disasters. The mercury intrusion experiment and uniaxial compression experiments were used to determine the changes in the pore structure and mechanical properties of coal after modified by surfactant. This work established six groups of water / surfactant / coal simulation systems with different concentrations. Based on the energy behavior and dynamics characteristics (interaction energy, relative concentration distribution, radial distribution function, mean square displacement) of each system, the effects of surfactants with different concentrations on the structural damage of coal were analyzed by molecular dynamics simulation, and the mechanism of coal structural damage was revealed. The results show that the SDS solution can significantly reduce the mechanical strength of the coal. When the solution concentration is 0.6%, the degree of damage to the coal structure is the maximum. SDS molecules can be detected at the water / coal interface. SDS molecules are adsorbed to the coal surface through intermolecular interactions, and $-SO_3$ groups are preferentially adsorbed to the oxygen-containing functional groups on the coal surface. The difference in SDS adsorption on the coal surface is caused by the difference in the number and spatial distribution of alkyl chains in the SDS molecule. The main modification mechanisms of surfactants on coal are that when SDS is adsorbed on the coal surface, a large number of secondary pores and cracks are generated on the surface and inside of the coal, and cracks are formed under the action of tensile stress. The cracks continue to expand, extend, which ultimately promotes damage to the coal structure. The results are expected to provide a theoretical basis for the structure damage of coal modified by surfactant, and provide a new method for the prevention of rockburst disasters and gas outburst control.

Introduction

The geological conditions of coal reservoirs in China are complicated [1–2]. Because of the stress of geological structure, the preexisting fissures of coal seam become narrow or impassable, which makes the pore and fissure structure of coal seam complicated and compact [3–4]. The complex structural characteristics of coal seam directly lead to the unrapid discharge of free gas in coal body, the low efficiency of gas extraction, which seriously limits the development of coal-bed gas in China[5]. At the same time, the complex structure of the coal seam also causes causes rock bursts and gas disasters, which endangers people's life and property safety[6–8].

In order to improve the efficiency of gas extraction and prevent the disaster of impact ground pressure, the modification of the physical and mechanical characteristics and structure of coal body has become the focus of current research. Researches[9–12] has confirmed that to some extent, coal seam water infusion can prevent coal and gas outburst. But the surface tension of most coal in China is lower than that of water, the wetting angle of water to coal is about 60 ~ 100°, it is difficult to spread water on the surface of coal, and it is difficult to achieve uniform wetting of coal seam[13–15]. Szymczyk et al.[16], Han Yixiu et al[17]. found that surfactant molecules have amphiphilic and can be adsorbed at the solid-liquid interface in aqueous solution, which can effectively reduce the interfacial tension and greatly enhance the spreading

ability of the solution on the solid surface. Therefore, many scholars studied the effect of surfactants on the wettability of coal in order to enhance the wettability of coal and reduce gas disasters. Crawford et al. [18] studied the effect of surfactant on the surface characteristics of different coal. It was found that add surfactant can obviously reduce the contact angle of coal and improve the wettability of coal. Paria et al. [19] studied the adsorption process of different types of surfactants at the solid-liquid interface. It was found that the physicochemical properties of solid surfaces depend on the type of surfactants. Because most cationic surfactants are derivatives of organic amine, when the solution is in contact with the coal surface, it becomes acidic, the organic amines are easy to precipitate, and the solution loses its surface-active action[20]. Zhang et al.[21] studied the wettabiliby change of four anionic surfactants on coal tar pitch surface. It was found that the surfactants with straight chain alkane as hydrophobic group was easier to wet coal pitch than the surfatant with condensed aromatics as hydrophobic group. Therefore, anionic surfactants with straight chain alkanes as hydrophobic group are widely used in experimental studies.

In recent years, molecular dynamics simulations have been used to study microscopic interactions between chemicals and mineral surfaces[22–26].The adsorption processed and interfacial morphology of anionic surfactants with different concentrations on the surface of graphene nanoparticles were simulated by Sun et al.[27] who adopted molecular dynamics simulation. Li et al.[28] studied the adsorption of anionic surfactants at the oil-water interface by molecular dynamics simulation. It was found that the hydrophobic chain of surfactants could help to reduce the interfacial tension. At present, the research on the modification of coal by surfactants mainly focuses on the change of the wettability of coal, but the modification mechanism of surfactants on the mechanical properties and pore structure damage of coal is not clear.

The preliminary research[29] of the research group found that, the anionic surfactant sodium dodecyl sulfate(SDS) has the best modification effect on coal. Therefore, this paper takes Fuxin long flame coal as the research object and uses different concentrations of anionic surfactant to modify the structure of coal. The change of pore structure of coal modified by surfactant was determined by Mercury injection experiment, the change of mechanical characteristics of coal modified by surfactant was determined by uniaxial compression text. And six groups of water/surfactant/coal systems with different concentrations were simulated by molecular dynamics simulation method. Through quantitative analysis of energy and dynamic characteristics, the mechanism of structure damage to coal by surfactants were revealed. In addition, the molecular level research based on molecular dynamics simulation is expected to provide a theoretical basis for the structure of coal modified by surfactants and a new method for the prevention and control of impact ground pressure disaster and gas outburst.

Experiment And Simulation

1.1 Experimental Materials and Solutions

The coal used in the experiment was taken from Fuxin Pingan mine (the depth of the coal seam is 500-1000m). Collect coal samples in accordance with national standards (GB/T482-2008), put the collected samples into collection bags immediately and seal them to prevent pollution and oxidation. The coal

samples has the characteristics of original micropore, microfissure and dense structure. Process coal samples in the laboratory. Use JKZS-100 automatic coring machine and YBDQ-4 rock cutter to cut the coal into standard coal samples according to standards (DL/T5368-2007, GB/T50266-99), and remove the coal samples with obvious defects. Obtain the coal samples with the size of Ø50 mm×100 mm. Carry out sonic wave speed test on coal samples, and remove the coal samples with large wave speed dispersion (more than 2 ~ 2.5 km/s). Select the coal samples with good uniformity, save them and reserve them. In order to ensure the uniformity of coal samples, each group of coal samples should be drilled on the same coal seam as much as possible. The standard coal samples are shown in Fig. 1, and the industrial analysis and element analysis of the coal samples are shown in Table 1.

The reagent used in the experiment was anionic surfactant —sodium dodecyl sulfate (SDS) with the molecular formula of $C_{12}H_{25}$-OSO_3Na. SDS has good properties of emulsification, penetration, decontamination and dispersion. Ni et al[30] found that when the concentration of surfactant solution reaches a fixed value, the surfactant solution will wet the coal particles. Li et al[31] used only three concentrations of sodium dodecyl sulfate (0.05%, 0.20% and 0.40%) to act on coal mine dust, which resulted in a small concentration range and lack of representativeness. Therefore, in this experiment, the SDS solution concentration is set to 0 ~ 1.0% (the concentration gradient is 0.2%).

Table 1
Industry and elemental analysis of standard coal samples

Coal samples	**Industry analysis / %**				**Density(g/cm^3)**	**elemental analysis/%**			
Average value	Moisture	Ash	Volatile	Fixed carbon	1.46	C	H	O	N
	6.01	30.32	23.68	40.00		78.09	6.54	13.96	1.41

1.2 Experimental Methods

1.2.1 Modification Experiment

Three parallel standard coal samples in each group were immersed in SDS solution with concentration of 0%, 0.2%, 0.4%, 0.6%, 0.8% and 1.0%, respectively. The modification temperature is set as 25 ℃ and the modification time is 48 h.

1.2.2 Mercury Injection Experiment

Crush the standard coal samples which before and after the modification experiment into 5 ~ 7g pieces of about 1cm to minimize the influence of mineral components in the coal sample on the experimental results. Put the fragments in a drying oven at 105°C for 24 hours to be tested. The Au-to Pore 9510 automatic mercury porosimeter is used to test the pore structure. The maximum mercury inlet pressure is 413MPa,

and the mercury withdrawal termination pressure is 0.1MPa. The surface tension of mercury is 4.85×10^{-3} N/m, the contact angle between mercury and the coal sample is 140°, the pressure range of the instrument is 0.1 ~ 60000pa, and the range of the measured pore size is 3.0nm ~ 1000μm.

1.2.3 Uniaxial compression test

Yaw-2000 hydraulic servo testing machine is used to test the mechanical strength of coal samples. Put the coal sample in the center of the press bearing plate, adjust the position of coal sample and spherical seat to make the upper surface of the coal sample contact with the upper bearing plate evenly. Start the testing machine, apply the initial load, and check the working condition of the testing machine. After normal operation, load uniformly at the loading speed of 0.01mm/s until the coal sample is completely destroyed. Observe the failure mode of the coal sample and record the failure load value. Axial displacement control is used in the text.

1.3 Molecular Dynamics Simulation

1.3.1 Surface Model of Coal

The macromolecular structure of coal is very complex. Coal chemistry believes that coal is formed by "basic structural units" with similar structures connected by bridge bonds. In this paper, the macromolecular model of Fushun long flame coal[32] proposed by Shi et al. is quoted and the model is slightly improved. Comparing Fuxin long flame coal with Fushun long flame coal in reference [33], it was found that Fuxin long flame coal has higher aromatic hydrogen ratio and aromatic carbon ratio, more aromatic hydrocarbon and less aliphatic hydrocarbon. But coal macromolecules are similar in a certain range ,based on this, the macromolecular structure of Fushun long flame coal was adjusted to remove Ca atom in the original model, and the molecular weight of long flame coal macromolecule with molecular weight of 2981 was obtained, and the molecular formula was $C_{194}H_{195}O_{26}N_3$. Material Studio 8.0 software is used to establish the molecular structure model of Fuxin long flame coal macromolecule, SDS surfactant and H_2O. The Smart Geometry Optimization method is used to optimize the structure of the model to minimize the energy of the structure model and make the structure more stable. The optimized structure is shown in Fig. 2. Using the Construction tool in the Amorphous Cell module and setting the periodic boundary conditions of the Periodic Cell. Put 10 coal molecules into a 32.4Å×32.4Å×32.4Å (length×width×height) box at 298K, and the porosity of coal surface model was calculated to be 4.22%, which is close to the mercury injection experiment. The surface structure model and porosity expression of coal are shown in Fig. 3. In addition, in the established coal surface model, because the model involves a large number of atoms, the bottom two-thirds of the coal structure model is constrained, and the top third is in free state, and this restrictive method basically has no effect on the calculation results [34]. In Fig. 3 (d), the red part indicates that the atom is constrained, and the gray part indicates that the atom is in free state.

1.3.2 Water / Surfactant / Coal Simulation System

Established six groups of water/surfactant/coal simulation systems with different concentrations from to in order to study the influence of surfactant concentration on coal structure damage. The concentration of surfactant in the system is realized by changing the quantity of surfactant, and the number of SDS molecules in the system is 0, 2, 4, 6, 8, 10, respectively, and the number of coal and water molecules is 3 and 1000, respectively. The Amorphous cell module is used to establish the unit cells of coal, water and surfactant. According to the structure density of coal under normal temperature and pressure, the density of coal is 1.46g/cm^3, and the density of water and SDS surfactant are 1g/cm^3 and 1.09g/cm^3, respectively. Using the Build Layers tool to randomly integrate the unit cells into a box with three-dimensional periodic boundary conditions. The box size is 32.4Å×32.4Å×52.8Å, forming six groups of water / surfactant / coal simulation systems with different concentrations. A vacuum gap of 60Å was established to prevent the periodic boundary conditions from affecting the system. The six groups of systems I ~ VI are shown in Fig. 4.

1.3.3 Simulation Method

The molecular dynamics module is carried out in the Forcite module. Firstly, the water / surfactant / coal simulation systems were established and the smart Geometry Optimization method was used to minimize the energy consumption. After geometry optimization, to avoid local optimization, Anneal tool is used for annealing dynamics to minimize the global energy. The annealing kinetic parameters are set as follows: The COMPASS II force field was applied in all simulations[35], the system was equilibrated in a constant pressure-temperature (NPT) ensemble using a Berendsen thermostat and barostat[36–37], each complete annealing cycle consists of 5 heating ramps and 5 cooling ramps, for which the target temperature is gradually increased from the initial temperature (300 K) to a mid-cycle temperature (500 K) and then decreased again to the initial temperature[38], A van der Waals interaction cutoff of 12.5 Å was employed, and the Ewald summation method was used to account for the long-range electrostatic interactions[39], and the dynamic annealing optimization of 100ps, 5000 steps and 1.0fs time step is carried out. Then, the Dynamics tool is used to calculate the dynamics. The dynamic parameters are set as follows: The COMPASS II force field was applied in all simulations, the molecular dynamics simulations were run at the NVT (constant volume and constant temperature) ensemble level at 298 K using a Nose thermostat[40], and the dynamic simulation is carried out with 100ps, 10000 steps and 1.0fs time step. For each cycle system, the dynamic simulation process is repeated three times to ensure the repeatability of the simulation. Taking system IV as an example, the equilibrium configuration of SDS solution on coal surface and the aggregation state of SDS after simulation are shown in Fig. 5.

Results And Analysis

2.1 Results of mercury injection experiments

The results of mercury injection experiments show that the porosity of the coal samples after modified by surfactants have changed to varying degrees, and the pore structure will also change accordingly[41]. The pores in coal are usually divided into four categories according to Hodot[42] classification method, visible pores V_4 ($D > 1000$ nm), mesopores V_3 ($1000\text{nm} \geq D > 100$ nm), transition pores V_2 ($100\text{ nm} \geq D > 10$ nm), micropore V_1 ($D \leq 10$ nm). The relation between the pore size and the pore volume of the coal samples before and after modified by surfactants is shown in Fig. 6.

Figure 6 showed the pore size distribution characteristics of coal samples after modified by surfactants. It can be seen from Fig. 6, when the pore size is bigger than 100nm, the difference between the stage pore volumes is very small, when the pore size is less than 100nm, the difference between the stage pore volumes is more obvious, because high pressure is required for mercury to enter the pores. The changes of pore structure of coal samples by surfactants are mainly reflected in the micropores and transition pores (which were less than 100nm). In other words, holes with a pore diameter of less than 100nm are the main ones, they provide most of the pore surface area. Therefore, the surfactant can change the pore structure of the coal samples, the total pore volume of the coal sample are increased, and the secondary pores and fracture are generated, the pore structure of the coal was damaged. When the concentration of surfactant is 0.6 wt.%, the total pore volume of coal sample increases the most, when the concentration is greater than or less than 0.6 wt.%, the total pore volume of coal sample is less than the concentration of 0.6 wt.%.

2.2 Results of uniaxial compression text

The stress-strain curves numbered 0–3(0%), 0.2-1(0.2%), 0.4-2(0.4%), 0.6-1(0.6%), 0.8-2(0.8%), 1.0–1(1.0%) were selected to explore the influence of surfactant concentration on mechanical properties of coal samples. The results are shown in Fig. 7 and Table 2.

It can be seen from Fig. 7 that coal samples underwent compression phase, elastic deformation, yield and post-peak strain softening during uniaxial compression. It can be seen from Table 2 that with the increase of the surfactant concentration (< 0.6%), the peak strength and elastic modulus of coal samples decreased with a large amplitude, while the peak strain increased with a large amplitude. When the surfactant concentration continues to increasee (> 0.6%), the peak strength and elastic modulus will increase with a small amplitude, and the peak strain will decrease with a small amplitude. This is mainly because there are many vacant adsorption sites on the coal surface for the surfactant to occupy when the surfactant concentration is low in the initial stage. With the increase of surfactant concentration, more and more vacant adsorption sites for the surfactant to occupy until the adsorption reaches saturation. When the surfactant concentration is too high (0.6%), the surfactant will form multi-layer adsorption or micelles on the surface of coal, and the adsorption between surfactant molecules will weaken the adsorption of the surfactant molecules originally absorbed on the surface of coal, and the electrostatic interaction between them will also gradually weaken. Therefore, when the concentration of surfactant is 0.6%, the mechanical parameters of the coal sample change the most, and the surfactant has the best modification effect on the coal.

The essence of the change in mechanical properties of coal after surfactant modification is that the surfactant damages the coal structure. During the surfactant modification process, surfactant molecules are continuously adsorbed on the surface of coal and the minerals inside the coal from outside to inside, and the coal is damaged. The damage of coal is manifested by its brittle failure, the internal fissures are expanded quickly, they cross unite to form the macro cracks. In turn, the peak strength and elastic modulus of the coal are reduced, the peak strain is increased, and the structure of the coal is damaged.

Table 2
Effects of surfactants concentration on mechanical parameters of coal

Surfactants concentration(%)	**0**	**0.2**	**0.4**	**0.6**	**0.8**	**1.0**
Peak intensity(MPa)	19.40	15.71	13.13	6.18	6.65	6.82
Elastic Modulus(MPa)	949	738	570	174	226	240
Peak strain	0.0146	0.0149	0.0157	0.0215	0.0192	0.0189

2.2 Results of uniaxial compression text

The interaction energy between surfactant and coal surface in the water/surfactant/coal system can be used to evaluate the interaction strength between them[43]. The calculate formula is as follows:

$$E_{Int} = E_{Total} - E_{Sur} - E_{Coal} - E_{Water} \quad (1)$$

where E_{Int} is the interaction energy between surfactant and coal surface, kcal / mol, E_{Total} is the total energy of the water/surfactant/coal system, kcal / mol, E_{Sur} is the energy of the surfactant, kcal / mol, E_{Coal} is the energy of coal, kcal / mol, and E_{Water} is the energy of water, kcal / mol.

From the energy perspective, it can be seen that the interaction energy (E_{Int}) between surfactant and coal surface is negative, the interaction between the two is spontaneous, and the greater the interaction value is, the easier the reaction is[44]. The interaction energy (E_{Int}) is positive, the interaction between the two is difficult to work or cannot work. It is worth noting that the interaction energy calculated in this paper only represents the strength of the interaction between surfactant and coal, and doesn't represent the thermodynamic adsorption energy[45]. It can be seen from Table 3that the interaction energy value of System Ⅰ (without surfactant) is small, for − 31 kcal / mol, this means that the water molecules adsorbed on the surface of coal is unstable. When surfactant is added to the system, the interaction energy of the System Ⅱ, SystemⅢ, and SystemⅣ is increased. With the increase of surfactant concentration, the interaction energy is increased with a large amplitude, and the interaction energy of SystemⅣ and System Ⅴ are more than System Ⅲ, but less than System Ⅱ (-350.30kcal/mol). Therefore, the results of System IV is the most ideal.

Table 3
Interaction energy between surfactant and coal surface in simulation systems with different concentrations

System	E_{Total} / (kcal/mol)	E_{Sur} / (kcal/mol)	E_{Coal} / (kcal/mol)	E_{Water} / (kcal/mol)	E_{Int} / (kcal/mol)
□	−8654.59	0	2240.87	−10864.46	−31
□	−9747.99	−934.61	2244.71	−10884.62	−173.47
□	−9235.39	−374.14	2244.96	−10875.84	−230.37
□	−9214.85	−363.41	2248.45	−10746.59	−353.30
□	−10664.23	−1831.52	2251.41	−10746.02	−338.10
□	−10856.75	−2338.57	2235.79	−10701.99	−321.98

2.4 Relative concentration distribution

The relative concentration distribution can describe the distribution of material in a certain direction. The adsorption morphology and spatial distribution of different concentration surfactants on the coal surface are explained by analyzing the relative concentration distribution of water / surfactant / coal system on the Z axis perpendicular to the coal surface[46]. The relative concentration distribution of the Systems □~□ is shown in Fig. 8, the peaks in the Figure indicate the concentrated position of the molecule or atom.

We can see from Fig. 8(a) that the relative concentration distribution of coal is relatively stable, both in the range of 0 ~ 6.5 nm, and it is almost unaffected by the surrounding environment. There is a little overlap between the relative concentration distribution of water molecules and coal, which indicates that there is a certain adsorption between coal and water molecules, but the adsorption is weaker. When surfactants are added in the system, it can be seen from Fig. 8(b) ~ Fig. 8(f), the spatial distribution range of surfactants with different concentrations are 4.98 ~ 9.12 nm, 5.63 ~ 9.20 nm, 7.22 ~ 8.03 nm, and 5.15 ~ 8.55 nm, respectively. Compared with the relative concentration distribution of surfactants in each system, system II has a wide distribution range, which indicates that there is a small adsorption between surfactant and coal surface in system II. The adsorption between surfactant and coal surface in different systems is as follows: IV > V > VI > III > II > I.

2.5 Radial distribution function (RDF)

Radial Distribution Function is a physical quantity that characterizes the microstructure and reflects the order of material aggregation. The arrangement of atoms in the SDS head group around C atoms and O atoms on the coal surface is studied by RDF to better understand the interaction between SDS and coal. The shape of RDF reflected the microstructure and the intensity of materials. The peaks are tip and high, which indicates that the order of atoms is good, the connection between atoms is tight, and the interaction

between atoms is strong. In addition, RDF can further explain and verify the competitive adsorption mechanism.

The radial distribution function represents the probability of other atoms B appearing in the spherical shell at $r+dr$ starting from an arbitrarily designated "center" atom A with a radius of r, expressed by $g_{A-B}(r)$[47].

$$g_{A-B}(r) = \frac{1}{4\pi\rho_B r^2} \cdot \frac{\mathrm{d}N_{A-B}}{\mathrm{d}r} \quad (2)$$

where $g_{A-B}(r)$ is the radial distribution function between atom A and atom B, ρ_B is average bulk density of SDS molecules, r is the distance between SDS molecules and coal surface, N_{A-B} is the average number of SDS molecules located between r and $r+dr$, A is the carbon or oxygen-containing functional groups of coal molecules, and B is the head group of SDS molecules.

Fig.9 showed the radial distribution function of the different concentration simulation System (□~□) about S atoms in the head group and O atoms in the oxygen-containing functional groups on the coal surface and the C atoms in the carbon-containing functional groups. The peak position of RDF curves represent the spatial adsorption distance, and the peak intensity of RDF curves represent the interatomic interaction intensity. For System II (Fig.9(a)), the first peak between S and O atoms was observed at r=0.38nm, the first peak between S and C atoms was observed at r=0.52nm, and the peak intensity of the former is higher than that of the latter. It can be seen that the -SO3 head group in the SDS molecule preferentially adsorbed on the oxygen-containing adsorption sites of the coal surface. It is because there are strong polar dipole interactions and electrostatic interactions between the $-SO_3$ head group in the SDS molecule and the oxygen-containing functional groups on the coal surface (such as -OH, -COOH, -C=O, and C-O-C, etc.). Compared with other systems (Fig.9(b)~Fig.9(e)), and combined the peak position and peak intensity in the RDF curve of each system. It can be seen that the position of the first peak between S and O atoms in System □ is the shortest (r=0.16nm), and the peak intensity is the highest. Similarly, the position of the first peak between S and C atoms in System □ is the shortest (r=0.25nm), and the peak intensity is higher than that of the other four systems. It can be seen from Fig.9 that the head groups of surfactant are preferentially adsorbed on the oxygen-containing functional groups of the coal surface. The interaction energy between the head groups of surfactant and the coal surface in different concentration systems is : □>□>□>□>□.

2.6 Mean square displacement of water molecules (MSD)

The adsorption of surfactants on the coal surface will affect the structure of the water phase and the movement of water molecules. Analyzing the mean square displacement and diffusion coefficient *(D)* of water molecules is to understand the dynamic characteristics of water molecules in the water/surfactant/coal system.

MSD is the statistical average of particle trajectories, which represents the average distance of the particle around another given particle, and it can characterize the diffusion behavior of water molecules[48–49].

MSD can be expressed as[50]:

$$MSD = \frac{1}{N}\sum_{i=1}^{N}\left[r_i(t) - r_i(0)\right]^2 \quad (3)$$

where, N is the number of diffusion molecules, $r_i(t)$ and $r_i(0)$ are the position vectors of the particles at time t and time $t = 0$, respectively.

The diffusion coefficient can reflect the migration speed. According to Einstein's equation [51–52], the expression of the diffusion coefficient D is:

$$D = \frac{1}{6N}\lim_{t\to\infty}\frac{\mathrm{d}}{\mathrm{d}_t}\sum_{i=1}^{N}\left[r_i(t) - r_i(0)\right]^2 \quad (4)$$

Combining formula (3) and formula (4), the relationship between MSD and diffusion coefficient D is:

$$D = \lim_{t\to\infty}\left(\frac{MSD}{6t}\right) = \frac{1}{6}K_{MSD} \quad (5)$$

where, K_{MSD} is the slope of the MSD curve.

MSD curves of water molecules in different concentration simulation systems are shown in Fig. 10. The MSD curves have different slops, and the K_{MSD} value of System I is smaller than the K_{MSD} value of System □~□. This shows that when surfactants are present, the adsorption of water molecules on the coal surface weakens and the diffusion of water molecules increases. The K_{MSD} value in the simulation system with different surfactant concentrations is, □>□>□>□>□>□. It is because the number and spatial distribution of hydrophobic alkyl chains of different concentration surfactants are different, and they have different hydrophobicity.

The diffusion coefficient of water molecules in the simulation system with different concentrations are shown in Table 4. The diffusion coefficient of system I is the smallest, which indicates that the diffusion behavior of water molecules on the coal surface is restricted. It is because the surface of coal contains a large number of polar groups, which have a strong hydrogen bond between them and water molecules to make the water molecules tightly adsorb on the coal surface. When surfactants are added, the diffusion coefficients of Systems □ to □ increase significantly, and the diffusion coefficient of System □ is the largest. This is mainly because the alkyl chain in the surfactant has a hydrophobic effect in the solution, which can repel the adsorption of water molecules on the coal surface, so that the -SO_3 head groups are adsorbed on

the vacancies on the surface of the coal. The greater the SDS concentration, the stronger the hydrophobic effect and the greater the diffusion coefficient. However, in System V and System □, the diffusion coefficient of water molecules is lower than that of System □. This is because when the SDS concentration is too high, there is a polar interaction between the SDS alkyl chains, which makes SDS itself form a tight adsorption layer. As a result, part of the -SO_3 head group extends out of the solution, reducing the adsorption of SDS on the coal surface. In summary, the dynamic characteristics simulation results are consistent with the energy behavior results, and both can describe the changes in coal pore structure and mechanical characteristics. The results fully verify the feasibility and accuracy of molecular dynamics simulation.

Table 4
Diffusion coefficient of water molecules in simulation systems with different concentrations

System	□	□	□	□	□	□
D / (10^{-4} cm^2/s)	0.927	0.980	1.120	1.569	1.463	1.229

Damage Mechanism Of Coal Structure

Before SDS solution modification, the original coal sample is composed of organic minerals and inorganic minerals. The inorganic minerals are composed of quartz particles, carbonate mineral particles, silicate mineral particles and sulfide particles. The mineral particles have good cementing properties. They are aggregated into a whole, there are intergranular pores between the aggregates, and the coal contains defects such as primitive micropores and microcracks. When surfactants are added, the SDS head groups are preferentially adsorbed to the coal surface through intermolecular interactions (mainly electrostatic interactions and van der Waals interactions), and SDS molecules formed a tightly arranged adsorption layer on the coal surface. The tightness of the adsorption layer on the coal surface is related to the modification conditions of SDS. When SDS was adsorbed on the coal surface, the microstructure of the coal changed, and the coal produced a large number of secondary pores and cracks. The previous research[53] of the research group found that the main reasons for these secondary pores and cracks were that the dissolution of organic minerals produced secondary pores, and the recrystallization and expansion of silicate minerals produced secondary cracks.

The damage process of coal microstructure after SDS modification are shown in Fig. 11. The original coal has a compact structure with a small number of pores and cracks inside and on the surface (Fig. 11(a)). After SDS modification, a large number of secondary pores and cracks appeared inside and on the coal (Fig. 11(b)), and they were connected to form cracks. Over time, existing cracks continue to extend to the inside of the coal to form large cracks, and at the same time, new cracks continue to occur on the surface and inside, which reduced the mechanical strength and caused local damage on the surface and inside (Fig. 11(c)). The number and width of cracks continue to increase, more pores and cracks are formed inside the coal, and the mechanical strength continues to decrease, which leads to damage to the overall structure of the coal (Fig. 11(d)).

Conclusion

(1) The results of mercury intrusion and uniaxial compression experiments show that there are more secondary pores and cracks are generated in the coal after surfactant modification, which can change the mechanical properties and cause damage to the coal structure. The peak strength and elastic modulus of coal first decrease and then slowly increase with the concentration increased.

(2) Molecular dynamics simulation results show that SDS molecules can be detected at the water/coal interface. SDS molecules are adsorbed to the surface of coal through intermolecular interactions, and -SO_3 groups are preferentially adsorbed on the oxygen-containing functional groups on the surface of coal. The difference in adsorption is caused by the difference in the number and spatial distribution of alkyl chains in SDS molecules. The degree of damage to coal structure by different systems is, □>□>□>□>□>□.

(3) There are a large number of secondary pores and cracks appeared inside and on the coal surface after SDS modification, and they were connected to form cracks. Over time, existing cracks continue to extend to the inside of the coal to form large cracks, and at the same time, new cracks continue to occur on the surface and inside, which reduced the mechanical strength and caused damage to the overall structure of the coal.

(4) The results of mercury intrusion, uniaxial compression experiments and molecular dynamics simulations fully demonstrate that anionic surfactants can promote structural damage in coal. The research results provide a theoretical basis for the surface active agent modified coal structure, and provide a new method for the prevention of rock burst disasters and gas outburst control.

Declarations

Data availability

Te primary data used to support the fndings of this study are available from the corresponding author upon request.

Acknowledgement

This work was supported by the National Key R&D Program of China (Grant no. 2017YFC1503100) and the NationalNatural Science Foundation of China (Grant no. 51474121).

Author contributions

Tis paper is the result of collaborative teamwork. He Chen: Data processing and paper writing. Laigui Wang□ Funding and ideas. Wenbo An□Samples preparation and experimental test. Na Zhao□Method and paper revision. All authors have read and approved the fnal manuscript.

Competing interests

Te authors declare no competing interests.

Additional information

Correspondence and requests for materials should be addressed to H.C.

References

1. Su, X., Lin, X., Liu, S., Zhao, M. & Song, Y. Geology of coalbed methane reservoirs in the Southeast Qinshui Basin of China. *International Journal of Coal Geology*, **62**, 197–210 (2005).
2. Cai, Y., Liu, D., Yao, Y., Li, J. & Qiu, Y. Geological controls on prediction of coalbed methane of No. 3 coal seam in Southern Qinshui Basin, North China. *Int J Coal Geol*, **88**, 101–112 (2011).
3. Cai, Y. *et al.* Pore structure and its impact on CH4 adsorption capacity and flow capability of bituminous and subbituminous coals from Northeast China., **103**, 258–268 (2013).
4. Su, X., Zhang, L. & Zhang, R. The abnormal pressure regime of the Pennsylvanian No. 8 coalbed methane reservoir in Liulin-Wupu District, Eastern Ordos Basin, China. *International Journal of Coal Geology*, **53**, 227–239 (2003).
5. Su, S., Chen, H., Teakle, P. & Xue, S. Characteristics of coal mine ventilation air flows. *Journal of Environmental Management*, **86**, 44–62 (2008).
6. Warmuzinski, K. Harnessing methane emissions from coal mining. *Process Safety and Environment Protection*, **86**, 315–320 (2008).
7. Pillalamarry, M., Harpalani, S. & Liu, S. Gas diffusion behavior of coal and its impact on production from coalbed methane reservoirs. *Int J Coal Geol*, **86**, 342–348 (2011).
8. Karacan, C. Ã., Ruiz, F. A., Cotè, M. & Phipps, S. Coal mine methane: A review of capture and utilization practices with benefits to mining safety and to greenhouse gas reduction. *International Journal of Coal Geology*, **86** (2–3), 121–156 (2011).
9. Huang, B., Liu, C., Fu, J. & Guan, H. Hydraulic fracturing after water pressure control blasting for increased fracturing. *International Journal of Rock Mechanics and Mining Sciences*, **48** (6), 976–983 (2011).
10. Cheng, W. *et al.* Research and practice on fluctuation water injection technology at low permeability coal seam. *Saf. Sci*, **50** (4), 851–856 (2012).
11. Colmenares, L. B. & Zoback, Mark, D. Hydraulic fracturing and wellbore completion of coalbed methane wells in the Powder River Basin, Wyoming: Implications for water and gas production. *AAPG Bulletin*, **91** (1), 51–67 (2007).
12. Zhao, D., Feng, Z. & Zhao, Y. Experimental study of effects on desorption of coal-bed methane(CBM) by high pressure water injection. *Chinese Journal of Rock Mechanics and Engineering*, **30** (3), 547–555 (in Chinese) (2011).
13. Xie, H. & Wang, K. Research on status and development trend about technology of dust control by injecting water in coal seam. *Journal of North China Institute of Science and Technology*, **12** (6), 10–13 (in Chinese) (2015).

14. Ni, G., Xie, H., Li, Z., Zhuansun, L. & Niu, Y. Improving the permeability of coal seam with pulsating hydraulic fracturing technique: A case study in Changping coal mine, China. *Process Safety and Environmental Protection*, **117**, 565–572 (2018).
15. Guo, Z., Hussain, F. & Cinar, Y. Permeability variation associated with fines production from anthracite coal during water injection. *International Journal of Coal Geology*, **147–148**, 46–57 (2015).
16. Szymczyk, K., Zdziennicka, A., Jańczuk, B. & Wójcik, W. The wettability of polytetrafluoroethylene and polymethyl methacrylate by aqueous solution of two cationic surfactants mixture. *Journal of Colloid and Interface Science*, **293** (1), 172–180 (2006).
17. Han, Y., Mei, Y., Wei, Y. & Zhou, H. Advance on Wettability of Surfactant Solutions[J]. *Chinese Journal of Colloid & polymer*, **30** (3), 133–136 (in Chinese) (2012).
18. Crawford, R. & Mainwaring, D. The influence of surfactant adsorption on the surface characterisation of Australian coals., **80** (3), 313–320 (2001).
19. Paria, S. & Khilar, K. A review on experimental studies of surfactant adsorption at the hydrophilic solid-water interface. *Advance Colloid Interface Science*, **110** (3), 75–95 (2004).
20. Meng, J. *et al.* Effect of different concentrations of surfactant on the wettability of coal by molecular dynamics simulation. *International Journal of Mining Science and Technology*, **29** (7), 577–584 (2019).
21. Peng, Z. H. A. N. G., Wenlong, W. E. I., Xing, L. I. & Chang, H. Effects of four kinds of anionic surfactants on wetting of coal tar pitch surfaces. *Journal of China Coal Society*, **39** (5), 966–970 (in Chinese) (2014).
22. Harami, H. R. *et al.* Mass transfer through PDMS/zeolite 4AMMMs for hydrogen separation: molecular dynamics and grand canonical Monte Carlo simulations. *Int Commun Heat Mass Transf*, **108**, 104259 (2019).
23. Meng, J. *et al.* Effects of Surfactant Compounding on the Wettability Characteristics of Zhaozhuang Coal: Experiment and Molecular Simulation. *Tenside Surfactants Detergents*, **57** (5), 390–400 (2020).
24. Yu, H. *et al.* An investigation of the nozzle's atomization dust suppression rules in a fully-mechanized excavation face based on the airflow-droplet-dust three-phase coupling model. *Adv Powder Technol*, **29** (4), 941–956 (2018).
25. You, X. *et al.* Molecular dynamics simulations of nonylphenol ethoxylate on the Hatcher model of subbituminous coal surface. *Powder Technol*, **332**, 323–330 (2018).
26. Chen, J., Min, F. & Liu, L. The interactions between fine particles of coal and kaolinite in aqueous, insights from experiments and molecular simulations.Applied Surface Science2019;467–468, 12–21.
27. Sun, H. & Yang, X. Molecular simulation of self-assembly structure and interfacial interaction for SDBS adsorption on graphene. *Colloids and Surf A: Physicochem Eng Aspects*, **462** (23), 82–89 (2014).
28. Li, Y. *et al.* The array and interfacial activity of sodium dodecyl benzene sulfonate and sodium oleate at the oil/water interface. *J Colloid Interface Sci*, **290** (1), 275–280 (2005).
29. An, W. *et al.* Technology optimization of surfactant for modification of low permeability coal by response surface methodology. *Journal of Safety Science and Technology*, **14** (07), 120–127 (in

Chinese) (2018).
30. Ni, G., Li, Z. & Xie, H. The mechanism and reliefmethod of the coal seam water blocking effect (WBE) based on the surfactants. *Powder Technol*, **323** (1), 60–68 (2018).
31. Li, Q. *et al.* Surface physical properties and its effects on the wetting behaviors of respirable coal mine dus. *Powder Technol*, **233** (1), 137–145 (2013).
32. Shi, K. *et al.* Study of construction of Fushun coal macro molecule structural model by infrared spectroscopy. *Polym. Bull*, **15** (3), 61–66 (in Chinese) (2013).
33. An, W. *et al.* Analysis the structural characteristics of Fuxin Long flame coal based on FTIR and XRD experiments. *Polym. Bull*, **15** (3), 61–66 (in Chinese) (2013).
34. Zhang, Z., Wang, C. & Yan, K. Adsorption of collectors on model surface of Wiser bituminous coal: A molecular dynamics simulation study. *Miner Eng*, **79** (10), 31–39 (2015).
35. Sun, H. COMPASS: An ab Initio Force-Field Optimized for Condensed-Phase Applications Overview with Details on Alkane and Benzene Compounds. *J Phys Chem B*, **102**, 7338–7364 (1998).
36. Collell, J. *et al.* Molecular simulation of bulk organic matter in Type II shales in the middle of the oil formation window. *Energ Fuel*, **28**, 7457–7466 (2014b).
37. Ungerer, P., Collell, J. & Yiannourakou, M. Molecular modeling of the volumetric and thermodynamic properties of kerogen: Influence of organic type and maturity. *Energ Fuel*, **29**, 91–105 (2014).
38. Ru, X. *et al.* Experimental and computational studies on the average molecular structur e of Chinese Huadian oil shale kerogen. *J. Mol. Struct*, **1030**, 10–18 (2012).
39. Wender, I. Catalytic Synthesis of Chemicals from Coal. *Catal. Rev. Sci. Eng*, **14**, 97–129 (2006).
40. Tang, H. *et al.* Theoretical study on the interactions between the lignite monomer and water molecules. *Russ. J. Phys. Chem. A*, **89**, 1605–1613 (2015).
41. Fu, X. *et al.* Fractal classifification and natural classifification of coal pore structure based on migration of coalbed methane. *Chinese Sci Bull*, **50**, 66–71 (2005).
42. Hodot, B. B. *Outburst of coal and coalbed gas (Chinese Translation)*p. 318(China Industry Press, Beijing, 1966).
43. Niu, H. *et al.* Molecular dynamics simulations of liquid silica crystallization. *Proc Natl Acad Sci U S A*, **115** (21), 534853–535252 (2018).
44. Bhoi, S., Banerjee, T. & Mohanty, K. Molecular dynamic simulation of spontaneous combustion and pyrolysis of brown coal using ReaxFF., **136**, 326–333 (2014).
45. Rai, B. *et al.* A molecular dynamics study of the interaction of oleate and dodecylammonium chloride surfactants with complex aluminosilicate minerals. *J Colloid Interface Sci*, **362** (2), 510–516 (2011).
46. Liu, J. *et al.* Molecular dynamics simulations of binary mixtures of anionic/cationic surfactants at oil water interface. *Chin J Process Eng*, **19** (3), 533–543 (2019).
47. Kong, X. & Wang, J. Copper (II) adsorption on the kaolinite (001) surface: insights from fifirst-principles calculations and molecular dynamics simulations. *Appl Surf Sci*, **389** (32), 316–323 (2016).
48. Van Niekerk, D. & Mathews, J. P. Molecular dynamic simulation of coal-solvent interactions in Permian-aged South African coals. *Fuel Process Technol*, **92** (4), 729–734 (2011).

49. Zhang, J. *et al.* Molecular dynamics investigation of thermite reaction behavior of nanostructured Al/SiO2 system. *Acta Phys Sin*, **63** (8), 086401 (2014).
50. Zhang, J. *et al.* Combined Monte Carlo and molecular dynamics simulation of methane adsorption on dry and moist coal., **122** (15), 186–197 (2014).
51. Einstein, A. On the Movement of Small Particles Suspended in Stationary Liquids Required by the Molecular-Kinetic Theory of Heat. *Ann. Phys*, **322**, 549–560 (1905).
52. Tao, C. *et al.* Molecular simulation of oxygen adsorption and diffusion in polypropylene. *Acta Phys. Chim. Sin*, **25**, 1373–1378 (2009).
53. An, W. & Wang, L. Mechanical properties and modification of coal under the ac-tion of surfactant. *Journal of China Coal Society*, **45** (12), 4074–4086 (in Chinese) (2020).

Figures

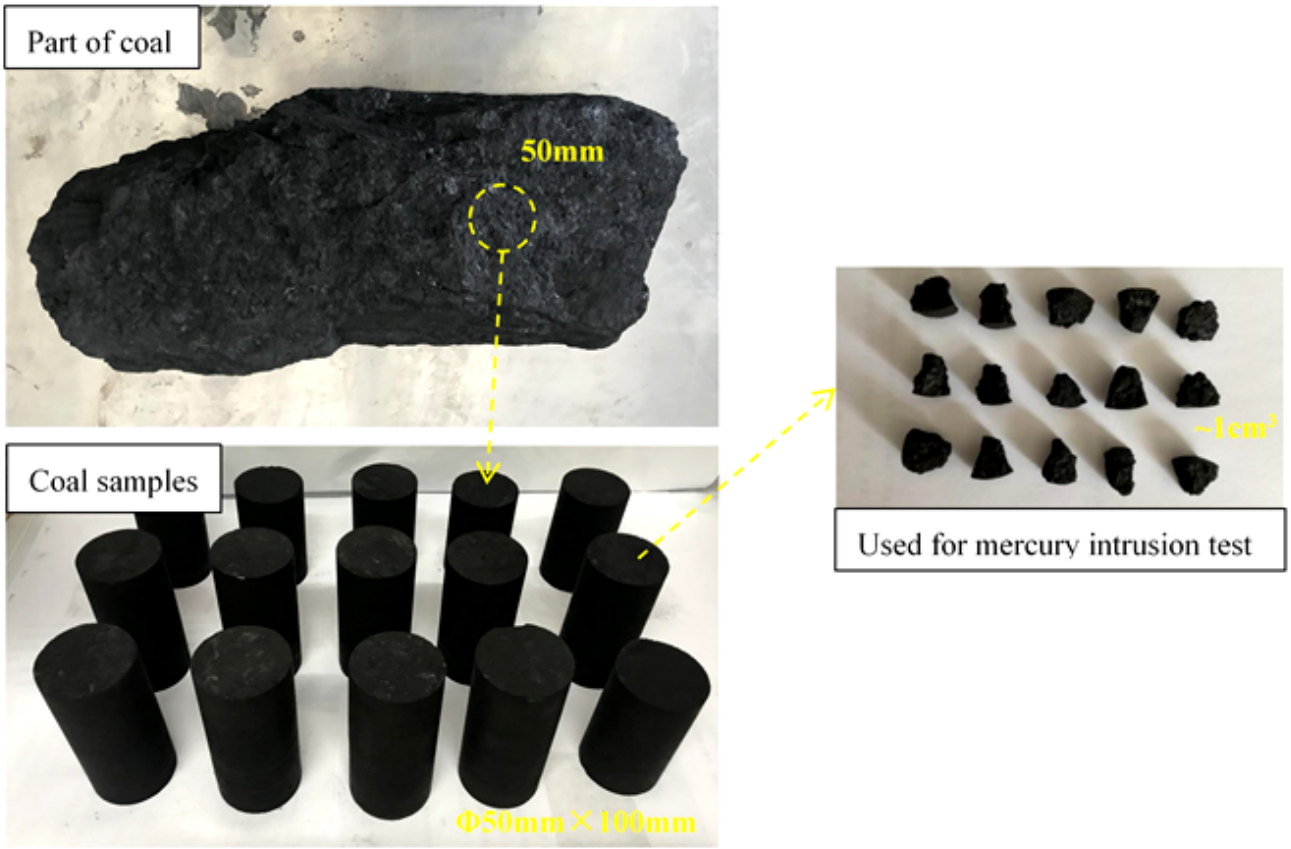

Figure 1

The standard coal samples

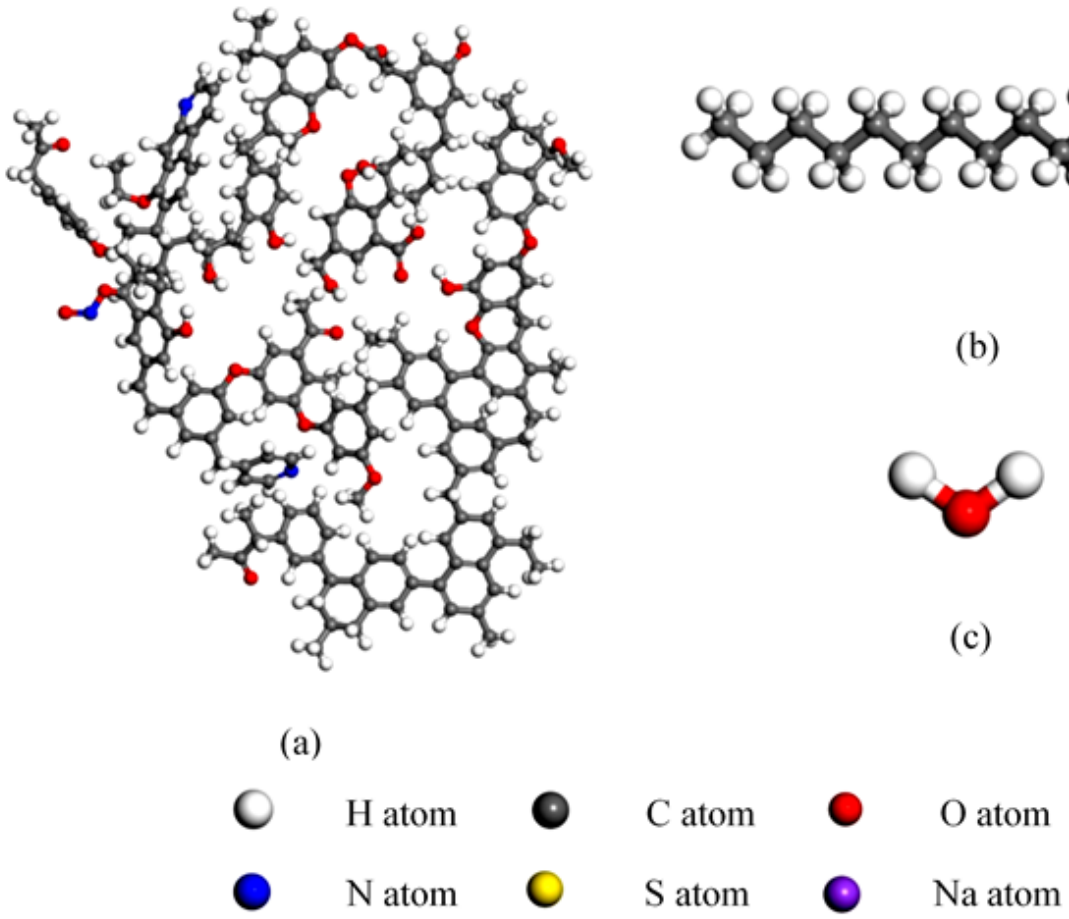

Figure 2

Optimization structure: (a)coal, (b)SDS, (c)H2O

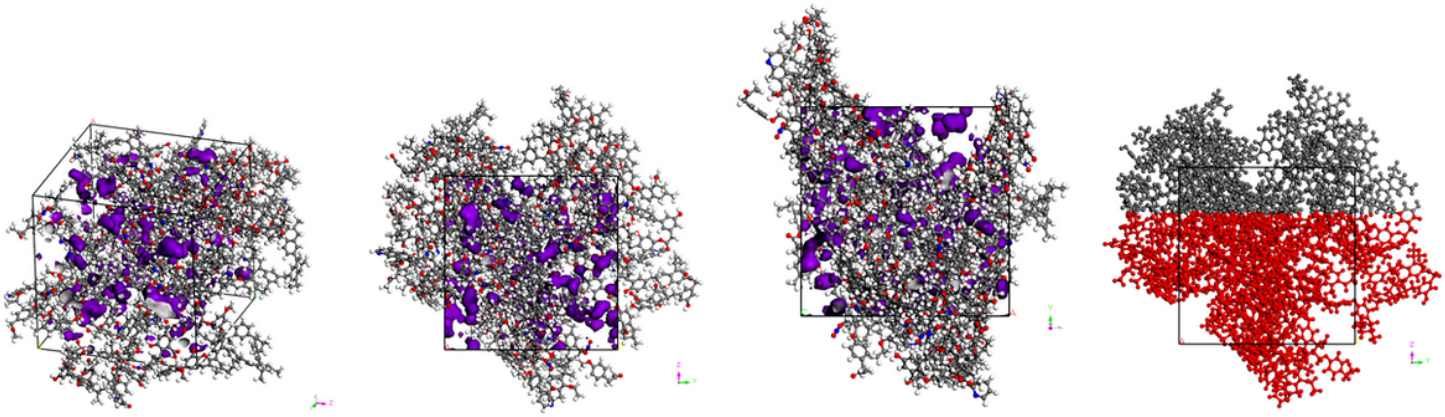

Figure 3

The surface structure model of coal with pores

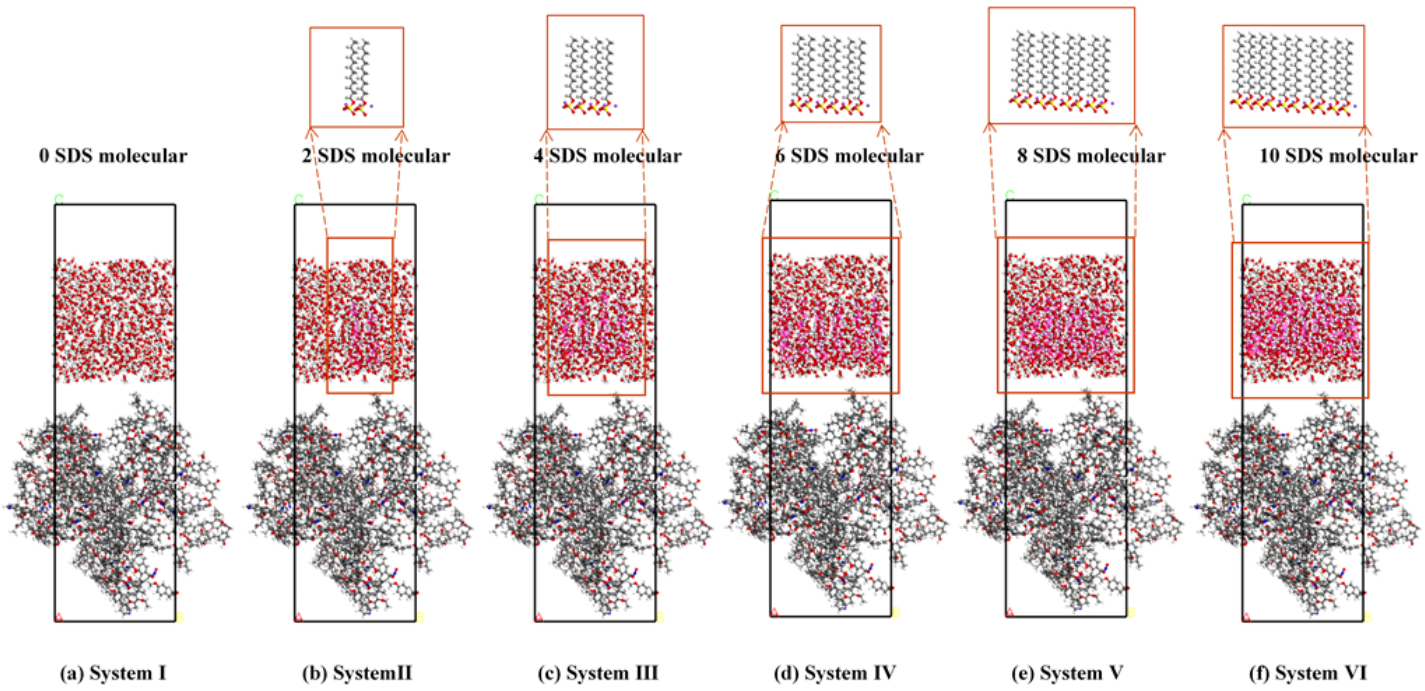

Figure 4

Water / Surfactant / Coal simulation system with different concentrations of ~

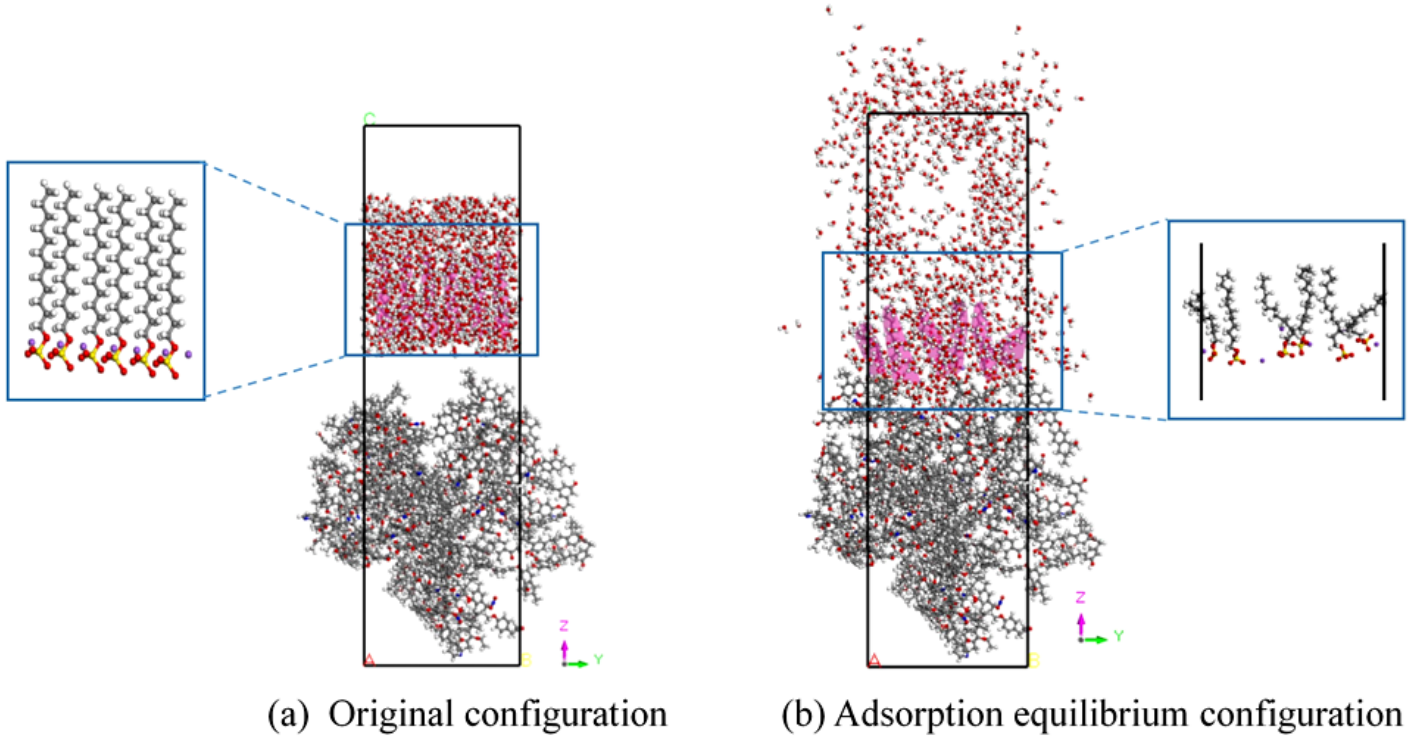

Figure 5

Adsorption of SDS solution on coal surface (System)

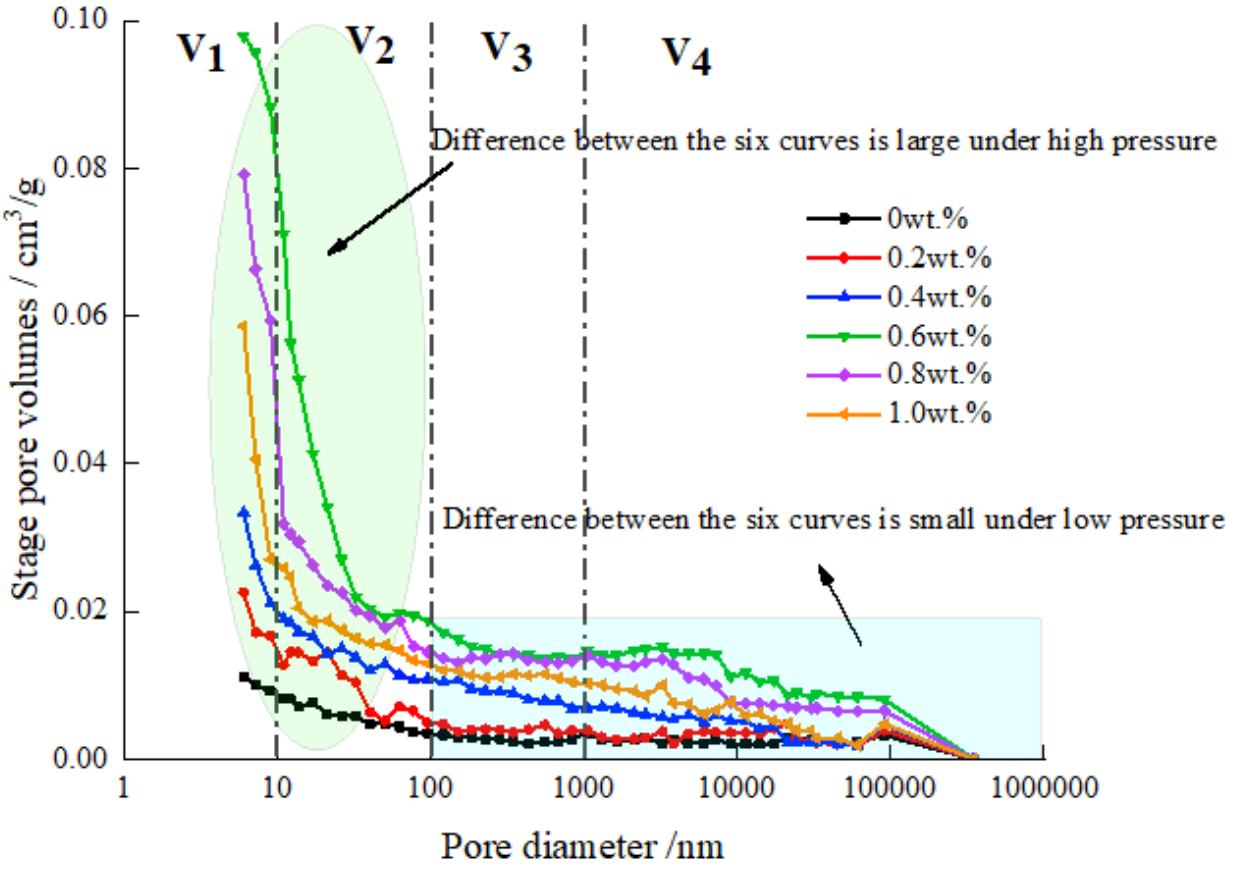

Figure 6

Pore size distribution characteristics of coal modified by SDS solutions with different concentrations

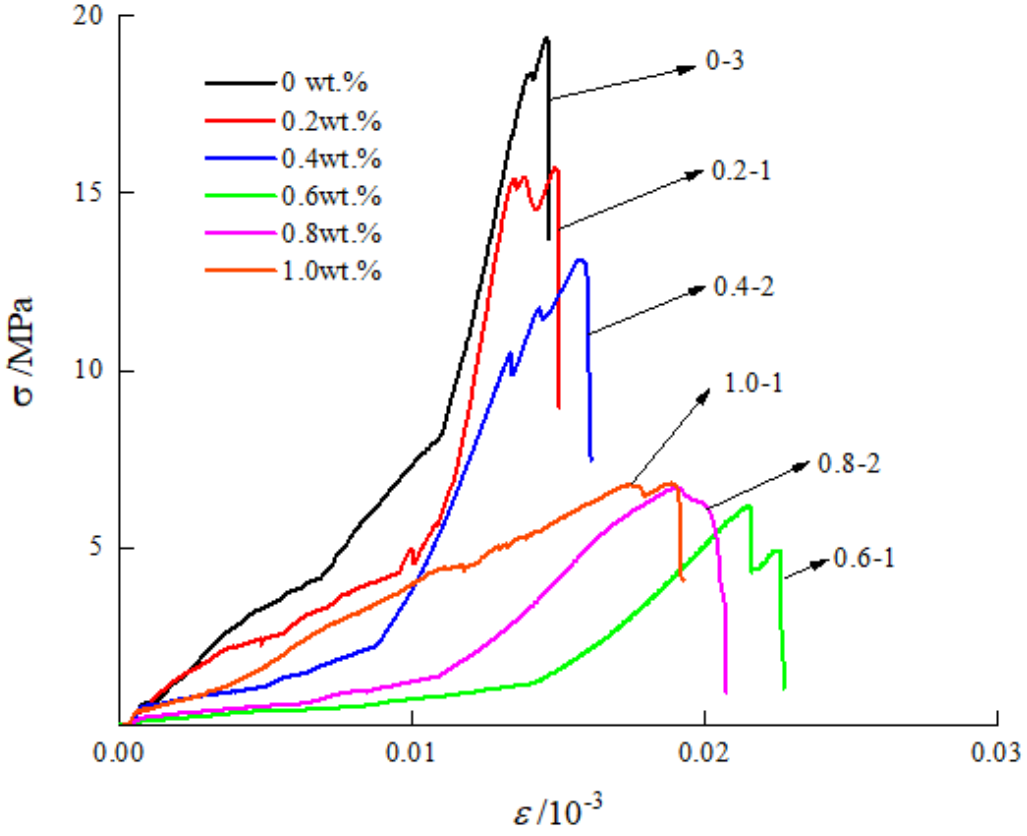

Figure 7

Stress-strain curves of coal modified by surfactant with different concentrations

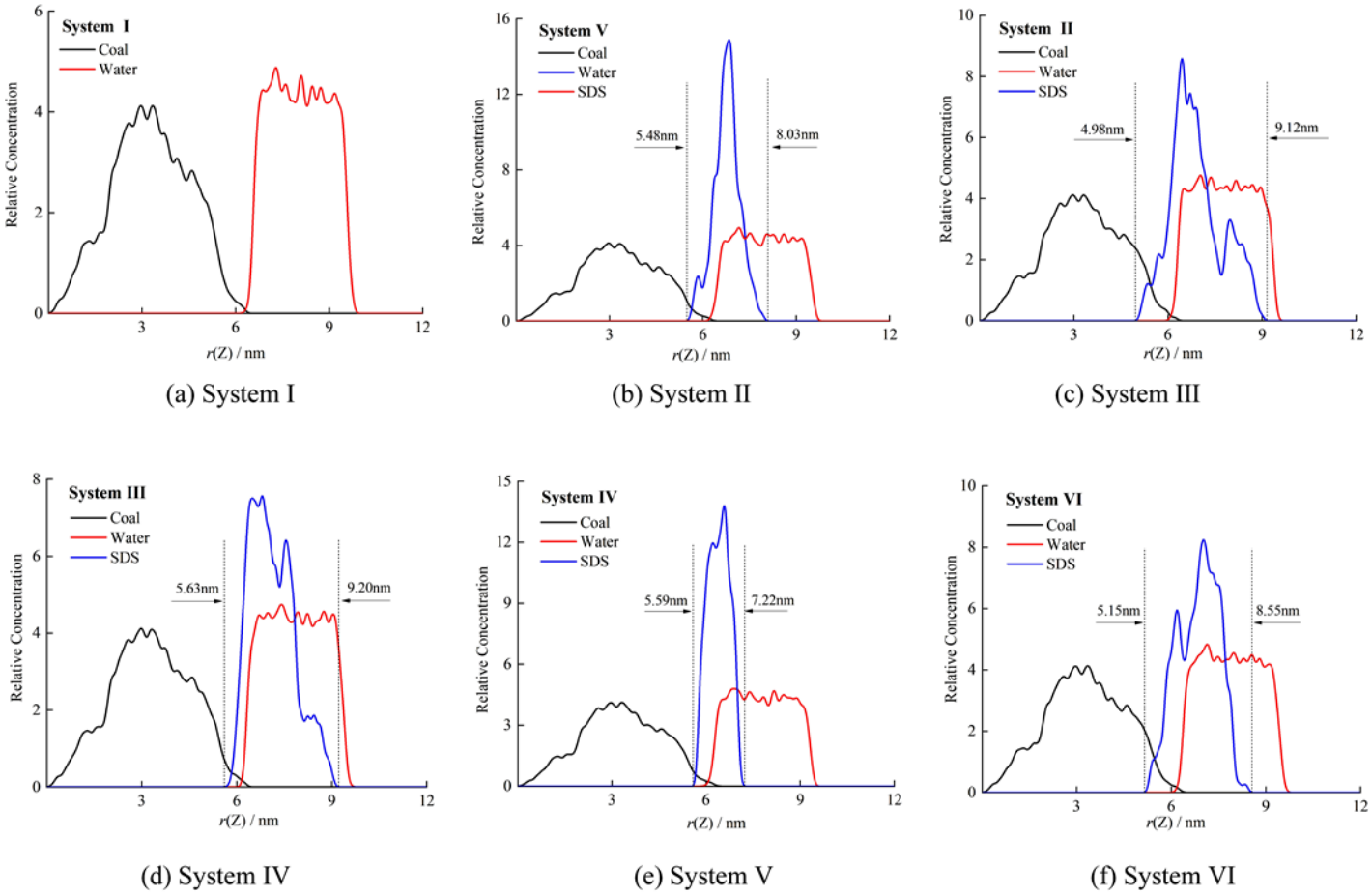

Figure 8

Relative concentration distribution of the simulation systems with different concentrations

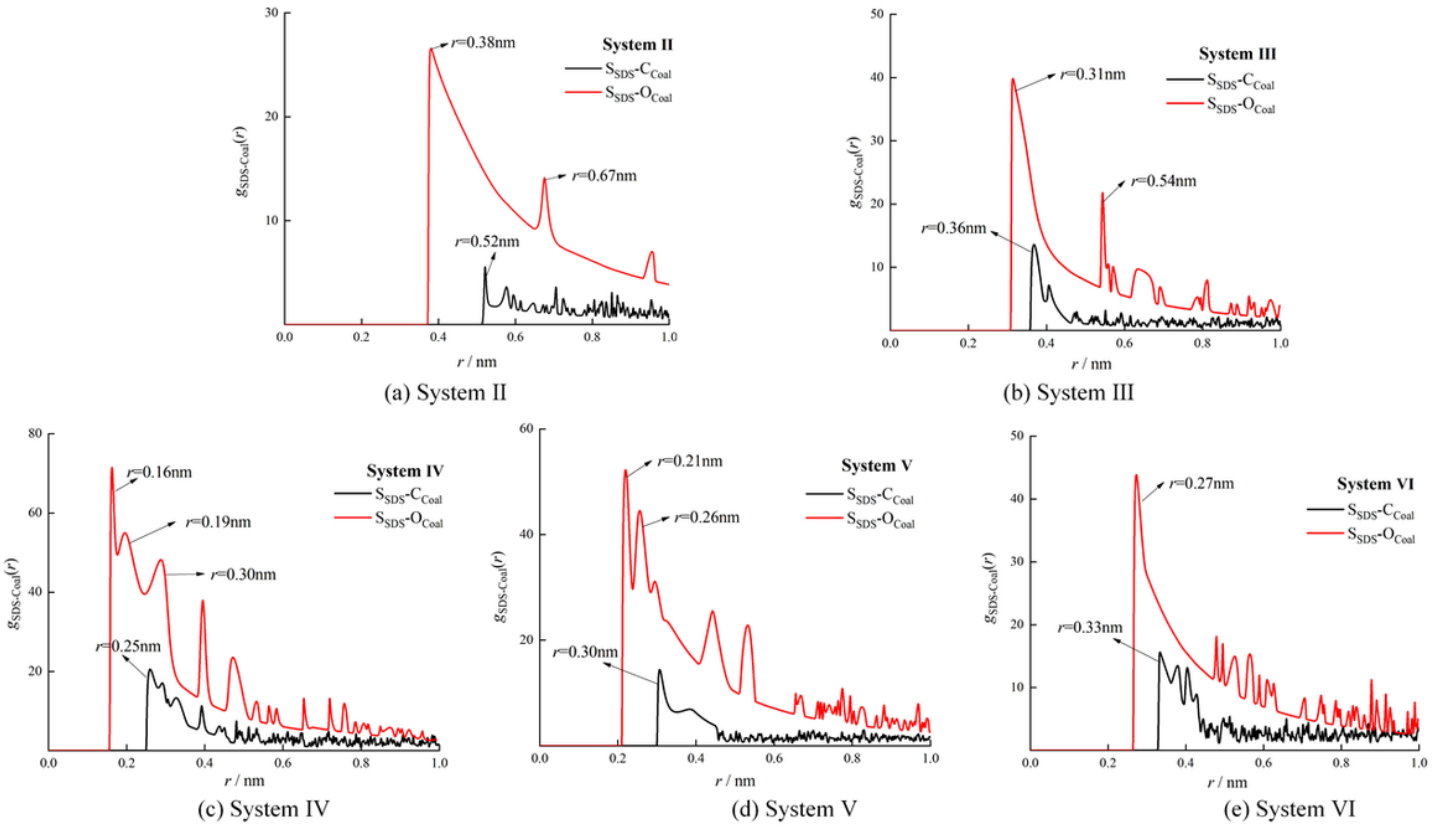

Figure 9

RDF of the sulfur (S) atoms around the carbon (C) and oxygen (O) atoms in different system (Ⅰ~Ⅵ)

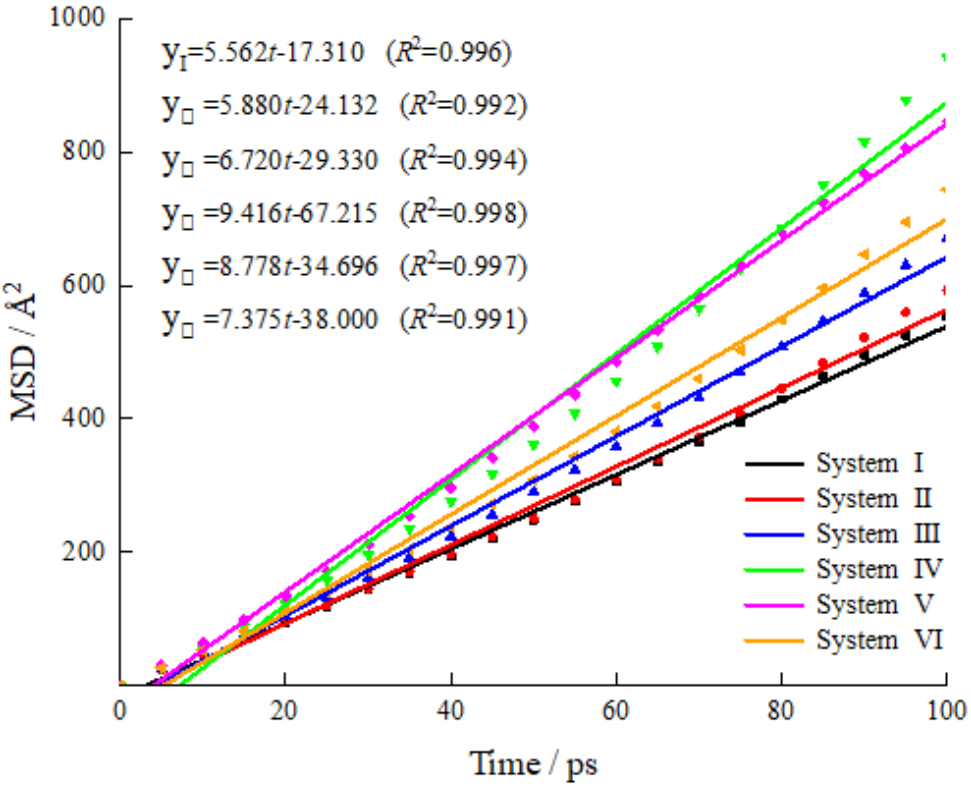

Figure 10

Mean square displacement of water molecules in simulation systems with different concentrations

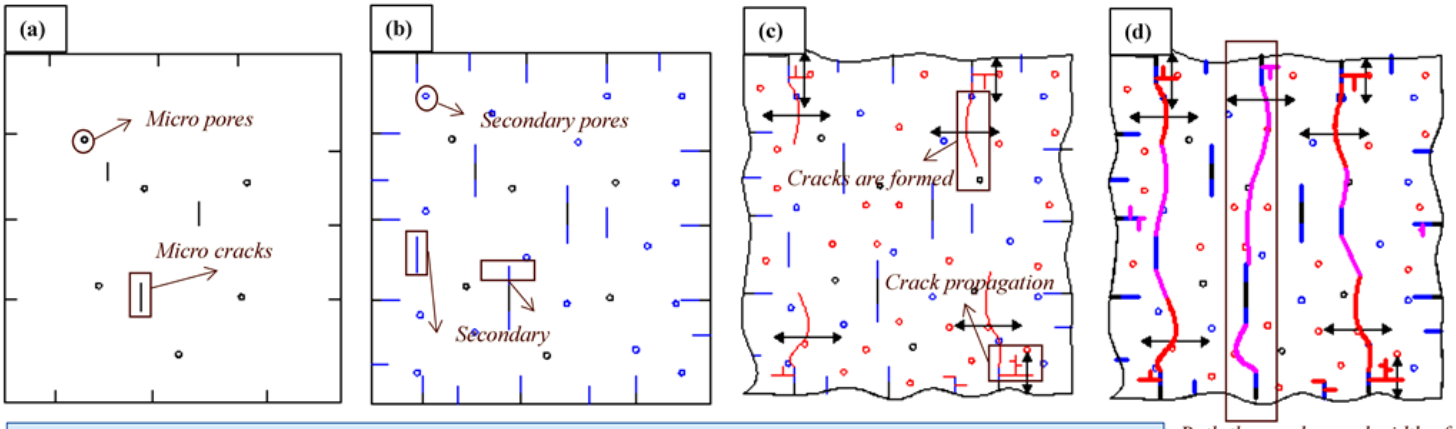

(a) Original coal sample has a compact structure with more micro pores and micro cracks.

(b) A large number of secondary pores and cracks are appeared after SDS modification.

(c) Cracks are formed over time, the mechanical strength of the coal decreased and local damage occurred.

(d) The number and width of cracks are increased, the overall structure of the coal is damaged.

Figure 11

Micro structure damage process of coal under the action of surfactant